Optik - International Journal for Light and Electron Optics 254 (2022) 168658

Contents lists available at ScienceDirect

Optik

journal homepage: www.elsevier.com/locate/ijleo

A comprehensive study on SILAR grown cobalt doped CdO thin films

Demet İskenderoğlu [a], Harun Güney [b], Muhammed Emin Güldüren [c,*], Mensur Albayrak [c]

[a] Kazım Karabekir Education Faculty, Department of Science Education, Atatürk University, Erzurum, Turkey
[b] Hınıs Vocational School, Department of Medical Services and Techniques, Atatürk University, Erzurum, Turkey
[c] Vocational School, Department of Electric and Energy, Ağrı İbrahim Çeçen University, Ağrı, Turkey

ARTICLE INFO

Keywords:
XRD
Thin films
Co doped CdO
SILAR
PL emission intensity and bandgap engineering

ABSTRACT

Herein, pure and cobalt (Co) doped cadmium oxide (CdO) thin films successfully deposited onto glass slides by successive ionic layer adsorption and reaction (SILAR) method. And, the structural, morphological, optical, and electrical properties were studied by employing X-ray diffraction (XRD), field emission scanning electron microscope (FE-SEM), Energy dispersive X-ray analysis (EDAX), Ultraviolet–visible spectroscopy (Uv-vis), Photoluminescence (PL) spectrum, I-V measurements for the produced samples. The XRD analysis uncovered that the CdO films exhibited cubic phase of cadmium oxide with the preferred orientation (111) plane. And, it showed that Co atoms successfully incorporated into the CdO lattices as no secondary phases were detected in the XRD spectra. The FE-SEM images displayed that the introduced impurities modified the surface morphologies. The EDAX analysis definitely proved the presence of the aimed materials (Cd, O, and Co) on the SILAR grown samples. The Uv-vis spectroscopy showed that optical energy bandgap enhanced from 2.5 eV to 2.93 eV as CdO nanostructures (NSs) doped with the different Co doping concentrations. The PL spectrum revealed that the luminescence characteristics of produced films were evidently influenced by the Co doping in the CdO NSs. Also, the resistivity of the produced samples was found to be decreased by the help of the I-V measurements.

1. Introduction

Transparent conducting oxides (TCOs) have been immensely studied by the researchers due to their broad utilizations in solar cells, gas sensors, photocatalysts, transparent electrodes, and flat panel displays [1–7]. These metal oxides such as indium oxide (In_2O_3), tin dioxide (SnO_2), zinc oxide (ZnO), and CdO are recognized to be as promising semiconductors as they have low resistivity and good transparency in the visible spectrum [8–11]. CdO attracts attention owing to the fact that it has a narrow direct bandgap of 2.2–2.5 eV with high carrier mobility. Also, it is an n type semiconductor with a face centered cubic crystal structure. CdO based thin films (TFs) have also been employed in optoelectronic devices like photovoltaics, optical communications, gas sensors, phototransistor, photodiodes, display technologies, etc. [12–15]. Furthermore, it is well established that structural, morphological, optical, and electrical features of metal oxides can be altered to enhance their certain characteristics for different device applications. Therefore, CdO has been previously doped with Co [1], Cr-Co [4], Ni-Al [5], Sn [6], Ba [9], Ag [10], Cu [11], Ce-Gd [12], Cl [16], etc., thus, its n-type

* Corresponding author.
E-mail address: megulduren@agri.edu.tr (M.E. Güldüren).

https://doi.org/10.1016/j.ijleo.2022.168658
Received 13 September 2021; Received in revised form 25 January 2022; Accepted 26 January 2022
Available online 29 January 2022
0030-4026/© 2022 Elsevier GmbH. All rights reserved.

conductivity and bandgap may be controlled accordingly. And, the convenient atomic radii of cobalt(0.065 nm) can be considered as an advantage when substituting Cd ions with the ionic radii of 0.095 nm in then CdO crystallites. Therefore, the impurity dopings can occupy the vacant sites in the CdO lattice, which may also lead to the production of films with stable physical properties.

Different methods have been executed for fabricating Co doped CdO TFs (Co:CdO), like spray pyrolysis [1,8], sol–gel method [17], pulsed laser deposition [18], chemical bath deposition [19,20], spin coating [21], SILAR [6,9,10], etc. Among these techniques, SILAR has emerged to be a economic, easy to use, and enabling homogeneous deposition of large TFs without no complicated vacuum procedures [6,9,10,22,23]. However, the reports on the impact of Co doping on the CdO NSs are very sparse in the literature, as well as the synthesis of Co:CdO nanostructures. There found to be only 6 studies in the web of science data base where "Co doped CdO" were identified as their title keywords. And, among them, there is only one other report [24] performed the SILAR technique to synthesize Co doped CdO TFs, which only conducted limited amount of analyses and concentrated more on the influence of annealing the CdO thin films.

Here, the coating of undoped and Co doped CdO NSs were presented by using the SILAR method which has emerged as a cost effective and uncomplicated coating technique. Also, the physical traits of the produced Co:CdO samples were asserted in order to reveal the effects of Co doping on the CdO NSs grown by the SILAR method. To our knowledge, the researches to this date have employed several deposition methods to fabricate the Co:CdO thin films, but the SILAR method has been barely employed. Thus, this study on the SILAR grown Co doped CdO NSs is aimed to shorten this gap in the literature, and examine the characteristics of the produced thin films for possible device applications.

2. Experimental

Pure CdO and Co:CdO TFs were synthesized on glass substrates at room temperature by the SILAR method. Before starting the deposition, a cleaning procedure needed to be followed to avoid possible imperfections on the glass slides, which can be decisive on the quality of the grown TFs. Therefore, the glass substrates were first immersed in dilute sulfuric acid (by 1/5 ratio), and then in deionized water (DI) for 5 min each, in an ultrasonic bath. After that, cationic and anionic precursors were prepared. For the cationic solution, cadmium nitrate tetrahydrate ($Cd(NO_3)_2.4\ H_2O$ - 98% purity) and cobalt nitrate hexahydrate ($Co(NO_3)_2.6\ H_2O$ - 99.9% purity) were acquired from Sigma-Aldrich and used without any further purification. The cationic solution was prepared from 100 ml of 0.1 M cadmium nitrate in DI water. And, 10 ml of 0.1 M cobalt nitrate solution prepared with DI water and added into the cationic solutions at different ratios which were 0%, 1% (0.25 ml), 2% (0.5 ml), and 4% (1 ml) labeled as (CdO), (CCO1), (CCO2), (CCO3), respectively. The anionic precursor was 400 ml of DI water which its pH value adjusted to 11.2 using ammonium hydroxide (29%) solution. A representative experimental diagram of the SILAR method is shown in Fig. 1. The cleaned glass substrates were first dipped in the cationic solution for 30 s at room temperature. Thereafter, the glass substrates were dipped in the anionic solution for another 30 s. And, this sequence completes one cycle of thin film deposition. For this particular set of thin films, this cycle repeated for 20 times. After that, all samples were annealed at 200 °C for approximately one hour. In addition to that, gravimetric weight difference method was employed to calculate the thickness of the grown samples [25]. Hence, the thicknesses were noted to be around 200 nm for all samples after 20 cycles of the SILAR deposition.

3. Results and discussions

Fig. 2 shows the XRD patterns of the undoped and Co-doped CdO films to determine the structural features of the grown CdO

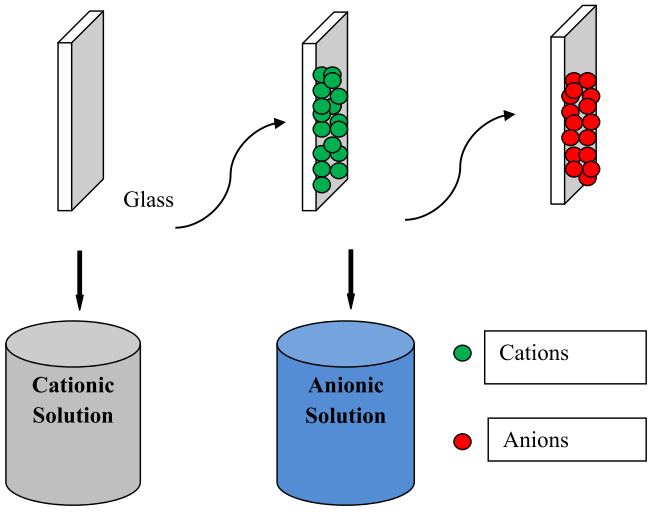


Fig. 1. Representative experimental diagram of the SILAR method.

samples. The diffraction angles were recorded in the range of 30° to 70°. All the thin films displayed face-centered cubic structure of CdO in polycrystalline nature (JCPDS Card no: 05–0640). The matching characteristic was reported for pure and cobalt doped CdO thin films prepared by spray and SILAR method in two separate works [1,24]. Also, Cr, Ba, Sn, Ag, Cu, Ni-Al, Ce-Gd, and La doped CdO thin films have been identified by the same JCPDS card, which were prepared by different deposition techniques [9–11]. The diffraction peaks observed at 2θ= 33.83°, 39.05°, 55.94°, and 66.32° were indexed as (111), (200), (220), and (311) planes of pure CdO sample, respectively. No other peaks detected corresponding to cobalt or the related phases of this dopant in the CdO nanostructrues. Hence, it may be interpreted as the Co atoms have been successfully integrated into the Cd sites. Besides, it can be seen that slight shifts occurred as a result of cobalt doping in the 2θ diffraction positions for the presented planes in Table 1. Thus, this may also be related to the incorporation of Co dopant in CdO lattice, and the differences between the ionic radii of Co^{2+} (0.065 nm) and Cd^{2+} (0.097 nm). Furthermore, Table 1 displays peak intensities (I) of the CdO samples. And, the intensity values of the (111) plane has been found to be decreased with increasing cobalt ratio in the CdO samples. This may also suggest that Co^{2+} dopants replace and Cd^{2+} ions in the lattice system. In addition to that, it can be clearly seen that the peak intensities (200), (220), and (311) for the produced CdO samples were notably altered by the Co doping. And, the intensity of the diffraction peaks for these different orientations was found to increase with increasing doping concentration which may point out that Co^{2+} ions incorporated in the lattice system were in interstitial sites in the CdO lattice [9]. Therefore, this can be interpreted as the cobalt doping can be substantial on the improvement of crystallinity as well as the nucleation and growth kinetics of CdO NSs [13]. And, this may also be a result of the internal stress created by the cobalt doping which affect the energy balance between distinct crystal plane orientations [26]. This was supported by the variation of microstrain with doping as displayed in Table 1. However, the intensity of the (111) plane decreased with higher Co doping level in the prepared CdO samples. This might be due to the fact that Co ions occupy the interstitial locations in the CdO crystallites [16].

The texture coefficient (*TC*) of the produced CdO TFs were evaluated by performing the formula given below on the XRD data [21];

$$TC_{hkl} = \frac{I(hkl)/I_0(hkl)}{N^{-1}\Sigma_n I(hkl)/I_0(hkl)} \quad (1)$$

where *N* is the number of reflections, $I_{0(hkl)}$ refers to the standard intensity of the (*hkl*) in the related JCPDS card data, $I_{(hkl)}$ gives the measured intensity of a plane (*hkl*), and n symbolize the count of diffraction peaks. To determine a preferential orientation, the texture coefficient ought to be greater than unity [6,12]. Hence, the texture coefficients of the preferential orientation (111) was greater than unity for all samples. And then, it decreased from 2.347 to 1.313 with increased doping percentage. On the other hand, the computed *TC* values for (200), (220), and (311) planes increased from 0.409 to 1.051, 0.366–0.843, and 0.878–0.970, respectively, as doping concentration increased. And, CCO2 sample had the second highest *TC* value for (200) plane after (111) plane. However, it was still lower than the *TC* value of CCO2 sample for (111) plane (1.313 >1.051). This opposite trend in the found *TC* values of (111) and (200) planes may be explained by the re-orientational effect in crystalline structure of CdO as reported previously [8]. Furthermore, Sahin et al. [24] conducted the first cobalt doped CdO by using the SILAR method, but no data can be found regarding the *TC* values of different orientation planes in the study.

In Table 1, the calculated crystallite sizes (*D*) were shown by employing widely recognized Debyee Scherrer's formula [10];

$$D = \frac{0,9\lambda}{\beta \quad cos\theta} \quad (2)$$

where β quantifies the full width at half maximum of the diffraction peak (FWHM), λ is the X-ray wavelength (1.5406 Å), and θ is ascribed to the Bragg's angle. In addition to this, the reported variations in peak intensities may refer to a modification in crystallite

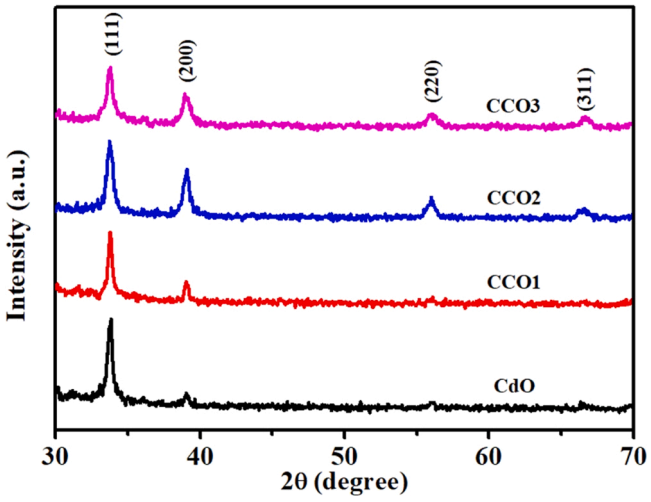


Fig. 2. XRD patterns of pure and Co doped CdO films.

Table 1
The XRD data and bandgap of the pure CdO and Co:CdO TFs.

Sample	Bandgap		2θ	FWHM	I	TC	D	δ	ε	d_0	d	a	a_{avg}	V
Name	(eV)	(hkl)	(°)	(°)		(hkl)	(nm)	(10^9/cm^2)	(10^{-3})	(Å)	(Å)	(Å)	(Å)	(Å)^3
		(111)	33,83	0,46	334	2347	165	37	23	2712	2648	4586		
CdO	2,5	(200)	39,05	0343	50	0409	218	21	15	2349	2305	4610	4628	99,114
		(220)	55,94	0,38	25	0366	185	29	11	1661	1642	4645		
		(311)	66,32	0439	39	0878	151	44	10	1416	1408	4671		
		(111)	33,78	0347	271	2227	219	21	18	2712	2651	4592		
CCO1	2,65	(200)	39,04	0355	82	0784	211	22	15	2349	2305	4611	4622	98,764
		(220)	56,01	0484	27	0462	145	48	14	1661	1641	4640		
		(311)	66,71	0659	20	0527	101	99	15	1416	1401	4647		
		(111)	33,74	0455	276	1313	167	36	23	2712	2654	4597		
CCO2	2,78	(200)	39,08	0493	190	1051	152	43	21	2349	2303	4606	4625	98,929
		(220)	55,99	0,62	85	0843	113	78	17	1661	1641	4642		
		(311)	66,58	0985	52	0793	67	220	22	1416	1403	4655		
		(111)	33,78	0,41	200	1441	185	29	21	2712	2651	4592		
CCO3	2,92	(200)	38,92	0,48	118	0989	156	41	21	2349	2312	4624	4627	99,045
		(220)	56	0736	40	0600	95	110	21	1661	1641	4641		
		(311)	66,66	0751	42	0970	88	128	17	1416	1402	4650		

size. As the doping percentage increased, the crystallite size corresponding to (111) plane also increased from 165 nm up to 219 nm which may suggest that Co doping enhances the crystallinity of CdO NSs. While the crystallite size increased, the FWHM values decreased with increasing the Co content which confirmed the Eq. 2 where β is inversely proportional to D. On the other hand, the calculated D values for (200), (220), and (311) planes decreased from 218 to 152 nm, 185–95 nm, and 151–88 nm, respectively, as doping concentration increased. The differences between the ionic radii of the Co^{2+} dopants (0.065 nm) and Cd^{2+} host metals (0.097 nm) may be the reason behind the modifications in the D values as well as the decrease in retarding force of nucleation induced by cobalt atoms in the crystal system. In addition to that, Velusamy et al. [1] found similar aftereffects of cobalt doping on the grain size of CdO NSs. In their study, the D values increased up to 0.5% of cobalt doping, and then it shrank as doping concentration rised. Sahin et al. [24] also noted that the D first increased with ~~co~~ cobalt doping, then it decreased as the CdO thin films doped with higher cobalt content. On the other hand, Mahasen et al. [14], Khalaf et al. [15], and El Sayed et al. [21] demonstrated that the grain size of the grown CdO NSs decreased right after the cobalt ions introduced to the CdO thin films. Although there are conflicting results on the aftermath of cobalt doping, it can be concluded that the higher level of cobalt content in the CdO crystallites will finally lead to the reduction of grain sizes.

The Bragg's law were employed to determine the interplanar distance (d) values of the prepared CdO NSs;

$$n\lambda = 2dsin\theta \tag{3}$$

where n is a positive integer, θ is the diffraction angle, and λ refers to the X-ray radiation ($\lambda = 1.5406$). Observed (d) and standard (d_0) interplanar distances of pure and cobalt doped CdO samples for (111), (200), (220), and (311) were presented in Table 1. Hence, the obtained d values matched well with the standard d_0 values listed in the JCPDS card which affirmed that the prepared samples by SILAR method belong to pure CdO crystallites. Lattice constant (a) and unit cell volume (V) were determined by performing the relations given below;

$$d = \frac{a}{\sqrt{(h^2 + k^2 + l^2)}} \tag{4}$$

$$V = a^3 \tag{5}$$

In Table 1, the a values for (111), (200), (220), and (311) planes varied from 4.586 to 4.597 Å, 4.606–4.624 Å, 4.640–4.645 Å, and 4.647–4.671 Å, respectively, as Co doping concentration changed. And, the average a_{avg} values found to be 4.628, 4.622, 4.625 and 4.627 nm for the pure CdO, CCO1, CCO2, and CCO3 thin films, respectively. The obtained average lattice constant for preferential orientation (111) was compatible with the standard value of CdO NSs in the JCPDS card (4.695 nm). Additionally, the lattice constants of CdO thin films for the preferred orientation along the (111) plane increased with the increase in Co doping concentration as shown in Table 1. This may be a result of a shift in the Bragg's angles of the (111) plane for the undoped and cobalt doped CdO samples which decreased from 33.83° to 33.74° [16]. Hymavathi et al. [27] anticipated that lattice constant of a material will decrease if doped with ions which have smaller ionic radius than the host material. This may be the reason of the initial decrease seen in the a_{avg} values of Co:CdO NSs since Co possesses smaller ionic radius than Cd.Moreover, the calculated V values were found as 99.114 Å^3, 98.764 Å^3, 98.929 Å^3 and 99.045 Å^3 for the pure CdO, CCO1, CCO2, and CCO3 thin films, respectively. In Table 1, the unit cell volume was noted to slightly decrease with the introduction of Co ions into the CdO lattices, but then it increased as the doping concentration increased. The observed unit cell volume values were also well matching with the given JCPDS card. Khalaf et al. [15] also found that both lattice parameter and unit cell volume decreased slightly with cobalt presence in the films, which may indicate the formation of the shortened interatomic spacing due to the interchange of larger Cd^{2+} ions, 0.095 nm,by smaller Co^{2+} ions, 0.065 nm.

Table 1 shows the dislocation density (δ) and microstrain (ε) which were evaluated from the given relations below [5];

$$\delta = \frac{1}{D^2} \tag{6}$$

$$\varepsilon = \frac{\beta \quad cos\theta}{4} \tag{7}$$

In Table 1, it can be seen thatthe dislocation density (or defect density) and microstrain values of preferred orientation (111) decreased with the addition of Co dopant ions. This decrement in the microstrain and dislocation density may be ascribed to the enhanced crystallinity of the prepared CdO thin films due to the increased order of atoms in the crystal lattice [1,8,24]. As these two found parameters showed opposite trend behavior with respect to the crystallite size, it can be said that the crystallinity of CdO samples can be enhanced by cobalt doping. On the other hand, in Table 1, the decrement/increment in the crystallite size, δ and ε values observed for the other orientation planes of the CdO TFs doped with Co may imply the fact that cobalt atoms occupy interstitial sites in the host lattice resulting in higher number of dislocations. Moreover, the δ and ε values corresponding to (200), (220), and (311) planes were given in Table 1 as cobalt doping concentration varied. On the contrary, these data were not supplied as extensively in any of the previous studies on the characterization of Co doped CdO TFs performed by Velusamy et al. [1], Mahasen et al. [14], Khalaf et al. [15], Nithin et al. [17], and Sahin et al. [24]. In Table 1, it can be seen that the δ and ε values of (200), (220), and (311) planes showed increment, in contrast with the related data for the preferential growth on (111) plane of the CdO NSs. Therefore, the crystallinity in (200), (220), and (311) planes can be expected to deteriorate as the defect density increased [1,15].

Fig. 3 shows the FE-SEM images and EDAX spectrums of the grown CdO TFs doped with various concentrations of Co (0%, 1%, 2% and 4%). The FE-SEM images of CdO thin films magnified 10,000 times. And, the synthesized CdO and Co:CdO samples showed porous nanoflake agglomerates where randomly shaped grain structures distributed throughout the surfacein the Fig. 3. Thomas et al. [20] and Sahin et al. [6,9] also noted the formation of nanoflakes in the grown CdO NSs which were deposited by hydrothermal and SILAR methods, respectively. Also, it can be seen that this shape of nanoscale morphology was retained after the cobalt doping. However, in the Fig. 3, it can be noticed that the fabricated CdO TFs may have lost their rather uniform distribution of nanoflake structures when the FE-SEM images of the pure and doped CdO films compared. Munawar et al. [4] also reported this type of diminished smoothness in the produced CdO thin film samples due to the added impurities. In the Fig. 3, the EDAX measurements were conducted to verify the presence of cobalt, cadmium, and oxygen elements in the produced Co:CdO by the SILAR method. It can be clearly seen in the EDAX spectra that O and Cd were the only main group of elements in the undoped CdO sample. In contrast to that, Co peaks were started to

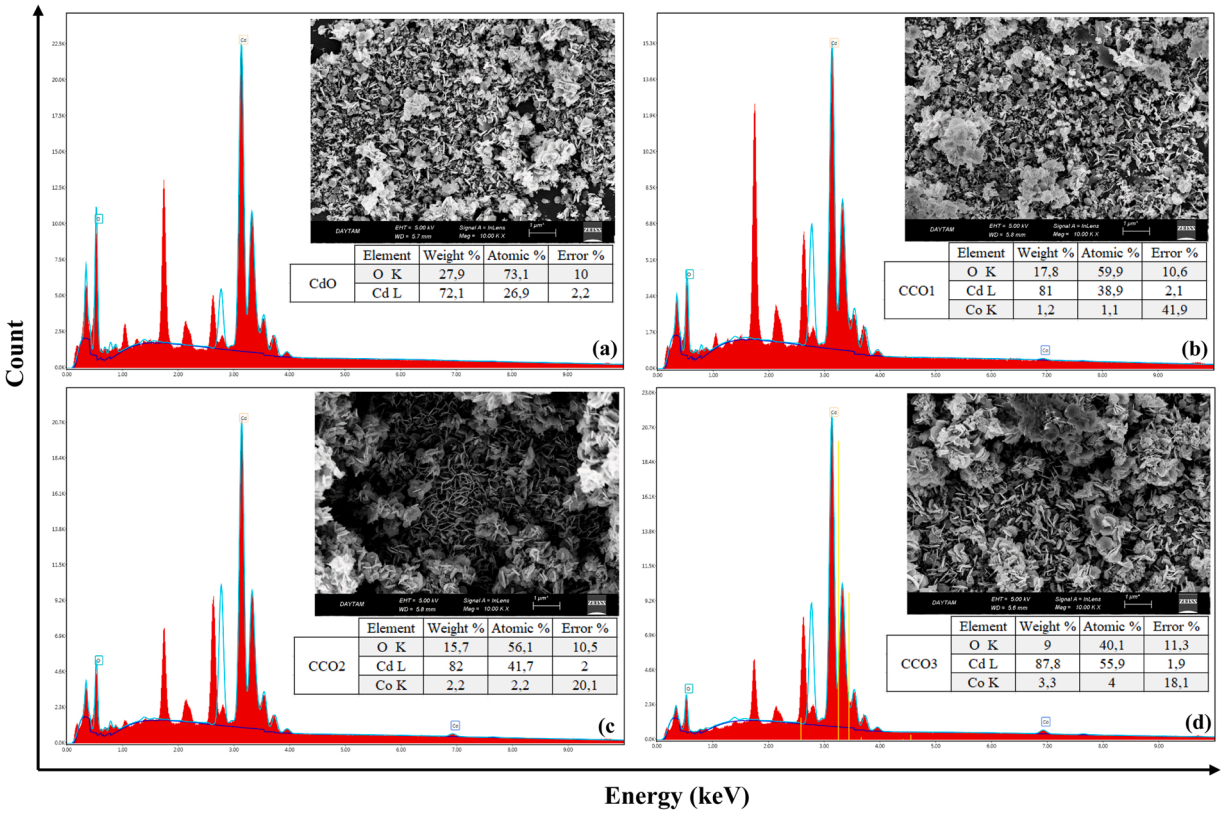


Fig. 3. The FE-SEM and EDAX analysis of undoped CdO and Co:CdO TFs.

appear after ~~doing~~ doping the CdO TFs with 1%, 2% and 4% of Co ions. Accordingly, the atomic percentage of Cd element increased with the higher Co doping concentration as tabulated EDAX data in the Fig. 3. However, atomic percentages of O in the prepared CdO films decreased from 73.1% to 40.1% as Co and Cd percentages increased. This may indicate the presence of oxygen vacancies formed by cobalt impurities in the grown samples, which also appeared in the modified PL spectras. Therefore, it can be said that the Co atoms were incorporated into O sites of CdO cyrstallites successfully by performing the SILAR technique.

Fig. 4 shows the UV–vis absorbance and reflectance spectra of the pure and Co doped CdO TFs in the range of 300–800 nm. The absorption spectra of all prepared samples indicate that the UV visible absorption edges of the undoped and Co doped CdO samples were located at 300 nm. The optical absorption of the prepared CdO thin film initially increased with Co doping up to 1% in the visible region, and then it decreased for the CdO samples with greater Co concentration. Therefore, it is evident that the absorbance decreased in the visible region for CCO2 and CCO3 thin films compared to pure CdO and CCO1 samples. Mahasen et al. [14] also found similar absorbance trend for Co doped CdO thin films, and they reported a continual decrease in absorbance values as doping concentration increased. However, in our work, the absorbance of produced TFs increased first with cobalt impurities, and then decreased due to the increased cobalt content in the CdO samples. Also, Yildirim et al. [3] and Nithin et al. [17] argued that the higher cobalt concentration (>4%) in the CdO lattice systems could lead to higher absorbance levels. From the Fig. 4, reflectance percentages of the prepared samples spectrum were altered by the different cobalt doping concentrations. Thus, the Fig. 4 clearly exhibits that the CCO3 sample reached the maximum optical reflectance, and the reflectance decreased for 1% and 2% Co doped CdO NSs. El Sayed et al. also stated that the reflectance of spin coated cobalt doped CdO thin films gradually increased as impurity percentage increased in the CdO nanocrystallites. However, in the present study, the reflectance of prepared CdO thin films differs from the previous work by displaying aperiodic increase as different amount of cobalt ions introduced to the CdO lattices.

The optical absorbance data can be used to determine the optical band gap energy of the produced CdO thin films. Hence, the band gaps of all samples were calculated using the well-known Tauc's equation given as;

$$\alpha = \frac{Absorbance}{t} \tag{8}$$

$$(\alpha h\nu) = A(h\nu - E_g)^{1/2} \tag{9}$$

where E_g is the band gap energy, h refers to the plank constant, t is the thickness of the thin film, $h\nu$ is the photoelectron energy, and A is constant. The E_g values were found to be 2.5 eV, 2.7 eV, 2.78 eV and 2.93 eV for CdO, CCO1, CCO2, and CCO3 nanoparticles as shown in Fig. 5. The obtained band gap for pure CdO agrees well with the previous reported values (2.2–2.6 eV) [28,29]. Besides, the Fig. 5 also points out a band gap broadening or blue shift of the calculated energy band gap as the doping amount of Co increases. This blue shift can be explained in terms of the Burstein-Moss effect which arises from the higher carrier concentration due to the increased doping ratios in the CdO crystal lattice [1,14,27]. Velusamy et al. [1] and Mahasen et al. [14] found similar optical energy band gaps for Co doped CdO thin films, which also showed a blue shift as cobalt doping concentration increased. And, the obtained band gaps in these works are all in good agreement with previous works. On the other hand, Khalaf et al. [15], Nithin et al. [17], and Sahin et al. [24], disclosed that the higher cobalt dopant contents lowered the optical energy band gaps of CdO NSs. However, the found band gap values of pure CdO films in these three previous studies were not in the estimated band gap range (2.2–2.6 eV) [28]of pristine CdO while the band gap of pure cadmium oxide sample found in this work were compatible within the suggested band gap of CdO. Moreover, there are other factors that may affect the band gap in semiconductors such as thickness, grain size, impurities, crystallinity, and deposition conditions which may prompt semiconductors to possess various optical energy band gaps [30]. Furthermore, the refractive index of the prepared CdO samples was calculated by employing the equation as follows [31];

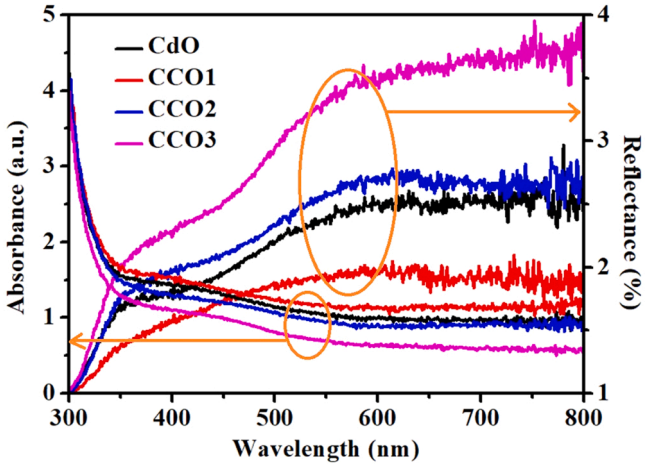


Fig. 4. The optical absorbance and reflectance spectrums of undoped CdO and Co:CdO TFs.

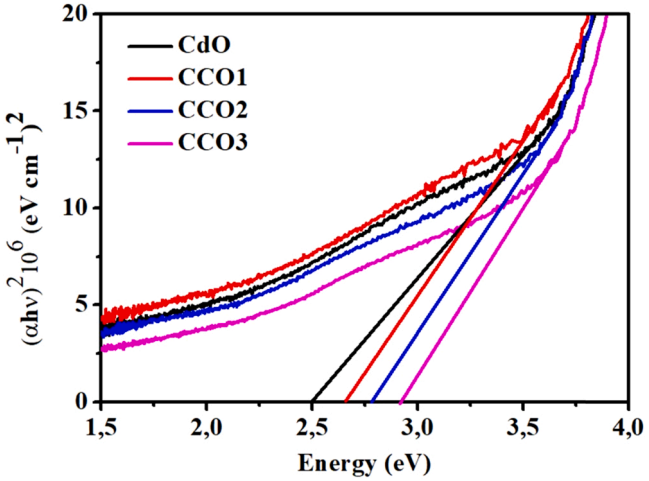


Fig. 5. The optical energy bandgap plots of the undoped CdO and Co:CdO TFs.

$$n = \left[\frac{1+R}{1-R}\right] + \sqrt{\frac{4R}{(1-R)^2} - k^2} \tag{10}$$

where R refers to reflectance data and k is known as the extinction coefficient ($k = \alpha\lambda/4\pi$). In Fig. 6, it was observed that the refractive index of the grown samples was affected by the cobalt doping. While the n values of 2% and 4% Co doped CdO samples increased, the refractive index of CdO sample with the lower doping percentage (1%) decreased with respect to the pure cadmium oxide film. Also, the n values of all samples increased with the increasing wavelength in general as shown in the Fig. 6. The obtained refractive index values were in good agreement with the previous reports [21,32]. El Sayed et al. [21] also showed that cobalt doping had an increasing effect on the n values of the CdO films; however, the refractive index of the CdO samples decreased as the wavelength increased in the relevant study.

Fig. 7 shows the PL spectra (recorded at an excitation wavelength of 325 nm) of the prepared CdO thin films in order to determine the emission spectrum which can provide more insights on the lattice defects of the CdO NSs due to the introduction of impurities. In the Fig. 7, it can be seen that there are three main PL emission peaks for pure CdO sample centered at 397 nm (3.12 eV), 518 nm (2.39 eV), and 718 nm (1.72 eV) which correspond to the violet, green, and red emission bands, respectively. These main peaks were outlined with the green lines as shown in the Fig. 7. And, there is also a weak visible peak located at 650 nm (1.90 eV). Menazea et al. [18] found that the peak 1 appeared at 397 nm (3.12 eV) can be attributed to the extended band emissions. And, they also noted that the strong emission peak at 518 nm (2.39 eV) can be ascribed to the electronic transitions of ionized oxygen vacancies due to the bottom of the conduction and top of the valence bands. Then, Ashaduzzman et al. [26] reported that the third peak at 718 nm (1.72 eV) refers to the red zone of electromagnetic spectrum which can be an evidence to the deep trap emissions occurredas result of oxygen

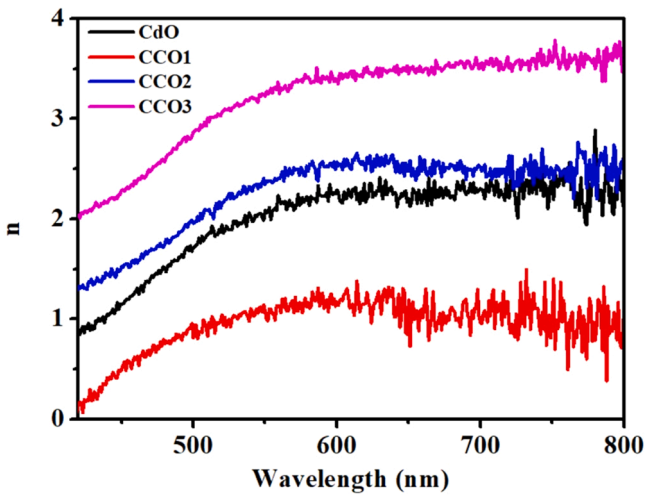


Fig. 6. The variation of refractive indexes for pure and Co doped CdO TFs.

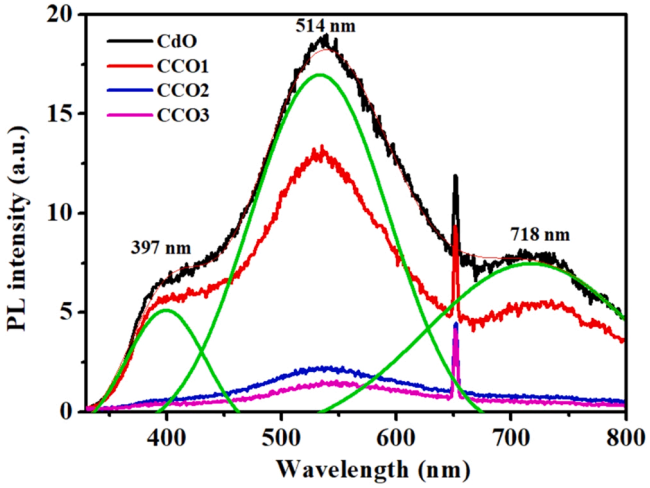


Fig. 7. The photoluminescence spectra of the undoped CdO and Co doped CdO TFs.

vacancies or lattice defects in the CdO thin films. Similar ranges of PL peak positions between 1.7 eV and 3.5 eV have been reported in literature as well [33,34]. However, the work presented here differs from the mentioned studies above by employing cost-effective SILAR method to dope CdO NSs with cobalt ions. And, this work gave a more collective look to PL spectra of CdO thin films while most of these previous studies focused only certain parts of the electromagnetic spectrum in their PL analysis or did not show any PL results at all. Moreover, it is observed that the PL emission intensity is notably reduced compared to that in the pure CdO thin film which can be related to the existence of interactions between the cobalt particles and CdO grains causing to alter the crystalline size as discussed previously in XRD results. Hence, these incidents may lead to reduce the electron-hole recombination which could aid the photocatalytic performance of the produced CdO thin films [2,35].

The I–V properties of unoped CdO and Co:CdO TFs were illustrated in Fig. 8. They show the Ohmic contacts for all the deposited films, which was made on CdO films by thermal deposition of aluminum (Al). The current of produced CdO NSs increased as cobalt doping level increased up to 1%, but thereafter decreased. Thus, the results of I-V assessment unveiled the order CCO1 > CCO2 > CCO3 > CdO for electrical conductivity (σ), and indicated that CCO1 has the highest conductivity values among all grown samples. And, this outcome may also grant the capability of the produced CdO samples as photocatalytic and energy storage devices. The increase in the conductivity of the CdO samples may be due to enhancements in crystallinity, increased cationic or anionic impurities, improved carrier concentration, decreased grain boundary and minimized structural deformations [1,16,24,30]. Besides, it can be seen that this increasing trend in conductivity can also be associated with the increment observed in the absorbance spectra as shown in the Fig. 4. Although Velusamy et al. [1] also noted similar electrical characteristics of CdO films as cobalt content increased, they employed spray pyrolysis method to grow their samples, which is prone to have difficulties such as oxidation, low yield and accurate growth temperature. Sahin et al. [24] conducted the SILAR method to produce Co doped CdO samples earlier, however they did not include I-V measurements in their work. Furthermore, cobalt element widely used as a dopant for other metal oxides such as TiO_2 and ZnO thin film samples, but the literature survey revealed that there have been no reports for the aftermath of Co integration over the electrical attributes of CdO NSs grown by SILAR method, yet.

4. Conclusions

In summary, the undoped CdO and Co:CdO TFs were successfully produced on the glass slides by using the SILAR method. Comprehensive analyses on the influences of cobalt doping on the physical characteristics of the prepared CdO samples were also presented here. In the XRD analysis,the *TC* of the (111) plane had the highest values of those observed due to the lower surface energy of this plane. However, it was observed that these *TC* values of (111) plane decreased due to the introduction of cobalt dopings. And, these impurities eventually caused deteriorations in crystalline quality owing to the misfit between the ionic radii of Co and Cd ions. The FE-SEM images demonstrated modified nanoflake structures as a result of Co doping in the CdO TFs. And, the EDAX measurements affirmed that the Co atoms integrated into the SILAR grown CdO samples. Also, the bandgap of the prepared TFs were widened from 2.5 eV to 2.93 eV. This may be a result of Burstein-Moss shift due to the added Co content into the CdO samples which may point out the existence of higher carrier concentration in the doped CdO TFs. And, the refractive index values of the SILAR grown CdO samples noted to be cobalt doping sensitive. The PL spectroscopy exhibited that the intensities of the obtained emission peaks were decreased with the increased Co concentration in the CdO NSs. Finally, the I-V analysis displayed that the introduced Co ions also influenced the resistivity of CdO TFs. Hence, it's shown that the lower Co doping led to the highest conductivity for the CdO films. Then, the conductivity decreased for the higher cobalt doping levels. Therefore, Co doped CdO NSs can be a worthy nominee for optoelectronic devices like LEDs, optical communications, smart windows, lasers, solar cells, photodiodes, etc., based on the tunable electrical and optical features shown in the present work.

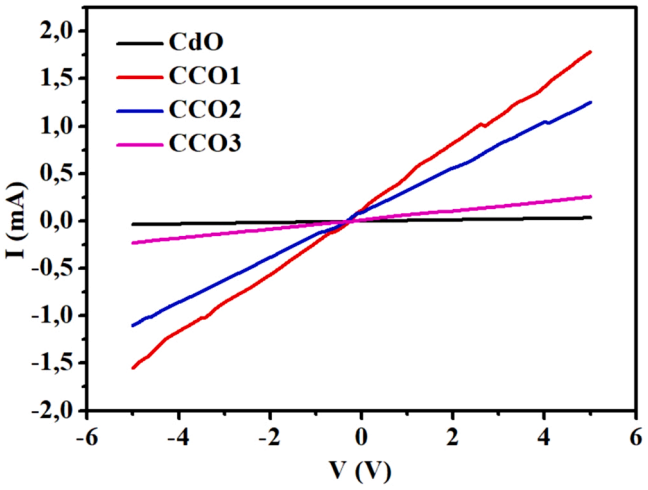


Fig. 8. The variation of I–V measurements of the undoped CdO and Co:CdO TFs.

Declaration of Competing Interest

The authors declare that they have no known competing financial interests or personal relationships that could have appeared to influence the work reported in this paper.

Acknowledgments

No funds, grants, or other support was received for the submitted work.

References

[1] P. Velusamy, R. Ramesh Babu, K. Ramamurthi, E. Elangovan, J. Viegas, M. Sridharan, "Gas sensing and opto-electronic properties of spray deposited cobalt doped CdO thin films.", Sens. Actuators B: Chem. 255 (2018) 871–883.
[2] Jing Liqiang, Wang QuYichun, Li Baiqi, Jiang Shudan, Yang Baojiang, Fu Libin, Fu Wei, Honggang, Sun Jiazhong, "Review of photoluminescence performance of nano-sized semiconductor materials and its relationships with photocatalytic activity.", Sol. Energy Mater. Sol. Cells 90 (12) (2006) 1773–1787.
[3] Ozlem Yildirim, Hanife Altintas, Arslan, Savaş. Sönmezoğlu, "Facile synthesis of cobalt-doped zinc oxide thin films for highly efficient visible light photocatalysts.", Appl. Surf. Sci. 390 (2016) 111–121.
[4] Tauseef Munawar, Muhammad Naveedur Rehman, Muhammad Shahid Nadeem, Faisal Mukhtar, Sumaira Manzoor, Muhammad Naeem Ashiq, Faisal Iqbal, "Facile synthesis of Cr-Co co-doped CdO nanowires for photocatalytic, antimicrobial, and supercapacitor applications.", J. Alloy. Compd. (2021), 160885.
[5] M. Banuprakash, B. Abhishek, Hrushikesh Acharya, Raghavendra Bairy, Shashidhara Bhat, H. Vijeth, M.S. Murari, A. Jayarama, Richard Pinto, "Structural, linear and nonlinear optical characterization of Ni and Al Co-Doped CdO semiconductor nanostructures for nonlinear optical device applications, Mater. Today.: Proc. 35 (2021) 396–404.
[6] B. Şahin, T. Taşköprü, F. Bayansal, "Bandgap variation of nanostructure tin doped CdO films via SILAR processing.", Ceram. Int. 40 (6) (2014) 8709–8714.
[7] A. Shameem, P. Devendran, V. Siva, M. Raja, S. Asath Bahadur, A. Manikandan, "Preparation and characterization studies of nanostructured CdO thin films by SILAR method for photocatalytic applications.", J. Inorg. Organomet. Polym. Mater. 27 (3) (2017) 692–699.
[8] G. Shanmugavel, A.R. Balu, V.S. Nagarethinam, "Preparation of cadmium oxide thin films by spray technique using perfume atomizer and effect of solvent volume on their physical properties.", Int. J. Chem. Mater. Res. 2 (9) (2014) 88–101.
[9] B. Sahin, Y. Gülen, F. Bayansal, H.A. Cetinkara, H.S. Güder, "Structural and optical properties of Ba-doped CdO films prepared by SILAR method.", Superlattices Microstruct. 65 (2014) 56–63.
[10] M. Yüksel, B. Şahin, F. Bayansal, "Nano structured CdO films grown by the SILAR method: Influence of silver-doping on the morphological, structural and optical properties.", Ceram. Int. 42 (5) (2016) 6010–6014.
[11] M. Benhaliliba, C.E. Benouis, A. Tiburcio-Silver, F. Yakuphanoglu, A. Avila-Garcia, A. Tavira, R.R. Trujillo, Z. Mouffak, "Luminescence and physical properties of copper doped CdO derived nanostructures.", J. Lumin. 132 (10) (2012) 2653–2658.
[12] L.L. Pan, G.Y. Li, J.S. Lian, "Structural, optical and electrical properties of cerium and gadolinium doped CdO thin films.", Appl. Surf. Sci. 274 (2013) 365–370.
[13] P. Velusamy, R. Ramesh Babu, K. Ramamurthi, E. Elangovan, J. Viegas, "Effect of La doping on the structural, optical and electrical properties of spray pyrolytically deposited CdO thin films.", J. Alloy. Compd. 708 (2017) 804–812.
[14] M.M. Mahasen, M.M. Soraya, E.L. Yousef, Gomaa Am Alid, E.R. Shaaban, Structural, thermal and optical analyses of cobalt-doped cdo thin films, J. Ovonic Res. Vol 15 (4) (2019) 247–260.
[15] A. Khalaf, M. Matar, W. Abdeen, "Tunable band gap and antiferromagnetic ordering in Co-doped CdO nanostructures.", J. Supercond. Nov. Magn. (2021) 1–11.
[16] K. Usharani, N. Manjula, A.R. Balu, V.S. Nagarethinam, "Characteristic analysis of nanostructured Cl-doped CdO thin films–doping effect.", Mater. Res. Innov. 20 (3) (2016) 182–186.
[17] K.V. Nithin, Kannan, M.R.M. Krishnappa, Synthesis and characterization of cobalt-doped cadmium oxide thin films prepared by sol–gel spin coating method, J. Phys.: Conf. Ser. vol. 1362 (1) (2019), 012118 (IOP Publishing).
[18] A.A. Menazea, M.Mostafa Ayman, Emad A. Al-Ashkar, "Impact of CuO doping on the properties of CdO thin films on the catalytic degradation by using pulsed-Laser deposition technique.", Opt. Mater. 100 (2020), 109663.
[19] L.R. de León-Gutiérrez, J.J. Cayente-Romero, J.M. Peza-Tapia, E. Barrera-Calva, J.C. Martínez-Flores, M. Ortega-López, "Some physical properties of Sn-doped CdO thin films prepared by chemical bath deposition.", Mater. Lett. 60 (29–30) (2006) 3866–3870.
[20] Paulose Thomas, K.E. Abraham, "Excitation wavelength dependent visible photoluminescence of CdO nanomorphotypes.", J. Lumin. 158 (2015) 422–427.

[21] A.M. El Sayed, Ali Ibrahim, Structural and optical characterizations of spin coated cobalt-doped cadmium oxide nanostructured thin films, Mater. Sci. Semicond. Process. 26 (2014) 320–328.
[22] Anbazhagan Murugan, Vadivel Siva, Abdulsamad Shameem, Sultan Asath Bahadur, Optimization of adsorption and reaction time of SILAR deposited Cu2ZnSnS4 thin films: Structural, optical and electrochemical performance, J. Alloy. Compd. 856 (2021), 158055.
[23] Anbazhagan Murugan, Vadivel Siva, Abdulsamad Shameem, Sultan Asath Bahadur, Effect of Zn on nanoscale quaternary Cu2ZnSnS4 thin film electrodes for high performance supercapacitors, J. Energy Storage 44 (2021), 103423.
[24] B. Sahin, F. Bayansal, M. Yüksel, H.A. Çetinkara, "Influence of annealing to the properties of un-doped and Co-doped CdO films.", Mater. Sci. Semicond. Process. 18 (2014) 135–140.
[25] D.S. Dhawale, A.M. More, S.S. Latthe, K.Y. Rajpure, C.D. Lokhande, "Room temperature synthesis and characterization of CdO nanowires by chemical bath deposition (CBD) method.", Appl. Surf. Sci. 254 (11) (2008) 3269–3273.
[26] M. Ashaduzzman, M.K.R. Khan, A.M.M. Tanveer Karim, M. Mozibur Rahman, Influence of chromium on structural, non-linear optical constants and transport properties of CdO thin films, Surf. Interfaces 12 (2018) 135–144.
[27] B. Hymavathi, B. Rajesh Kumar, T. Subba Rao, Structural, surface morphological and optical properties of Cr doped CdO thin films for optoelectronic devices, Mater. Today.: Proc. 2 (4–5) (2015) 1510–1517.
[28] I. Akyuz, S. Kose, E. Ketenci, V. Bilgin, F. Atay, Optical, structural and surface characterization of ultrasonically sprayed CdO: F films, J. Alloy. Compd. 509 (5) (2011) 1947–1952.
[29] Azadeh Tadjarodi, Mina Imani, Hamed Kerdari, "Application of a facile solid-state process to synthesize the CdO spherical nanoparticles.", Int. Nano Lett. 3 (1) (2013) 1–6.
[30] Wael Z. Tawfik, S.Khalifa Zaki, M.Sh Abdel-Wahab, Ahmed H. Hammad, "Sputtered cobalt doped CuO nano-structured thin films for photoconductive sensors.", J. Mater. Sci.: Mater. Electron. 30 (2) (2019) 1275–1281.
[31] Mujdat Caglar, Saliha Ilican, Yasemin Caglar, "Influence of dopant concentration on the optical properties of ZnO: Infilmsby sol–gel method.", Thin Solid Films 517 (17) (2009) 5023–5028.
[32] V. Ganesh, L. Haritha, H. Elhosiny Ali, A.M. Aboraia, Yasmin Khairy, H.H. Hegazy, V. Butova, et al., The detailed calculations of optical properties of indium-doped CdO nanostructured films using Kramers-Kronig relations, J. Non-Cryst. Solids 552 (2021), 120454.
[33] Rajini Murugesan, Karunakaran Marimuthu, Kasirajan Kasinathan, Maheswari Sathiah, Chandramohan Rathinam, "An Investigation of SILAR Grown CdO, Thin Films." Iran. J. Chem. Chem. Eng. (IJCCE) 38 (4) (2019) 11–17.
[34] Raghavendra Bairy, A. Jayarama, Suresh D. Kulkarni, M.S. Murari, H. Vijeth, "Role of Zn in tuning the band gap, surface morphology, photoluminescence and optical nonlinearities of CdO nanostructures for photonic device applications.", Mater. Res. Express 6 (9) (2019), 096447.
[35] Long Zhang, Lianhuan Du, Xiang Yu, Shaozao Tan, Xiang Cai, Peihua Yang, Yu Gu, Wenjie Mai, "Significantly enhanced photocatalytic activities and charge separation mechanism of Pd-decorated ZnO–graphene oxide nanocomposites.", ACS Appl. Mater. Interfaces 6 (5) (2014) 3623–3629.